

We are IntechOpen, the world's leading publisher of Open Access books Built by scientists, for scientists

6,900

Open access books available

186,000

International authors and editors

200M

Downloads

Our authors are among the

154

Countries delivered to

TOP 1%

most cited scientists

12.2%

Contributors from top 500 universities



WEB OF SCIENCE™

Selection of our books indexed in the Book Citation Index
in Web of Science™ Core Collection (BKCI)

Interested in publishing with us?
Contact book.department@intechopen.com

Numbers displayed above are based on latest data collected.
For more information visit www.intechopen.com



Aluminum Nitride (AlN) Film Based Acoustic Devices: Material Synthesis and Device Fabrication

Jyoti Prakash Kar¹ and Gouranga Bose²

¹*Department of Electronics Engineering, University of Tor Vergata, Rome*

²*Department of Applied Electronics and Instrumentation Engineering,
Institute of Technical Education and Research, Bhubaneswar, Orissa*

¹*Italy*

²*India*

1. Introduction

Enormous growth has taken place in electronics, especially in the field of RF communications towards the beginning of 21st century and continuously striving for better communication performance. Presently, the key concerns of RF communications is bandwidth, in the range of low/medium GHz range, to avoid frequency crowding, especially for wireless communication mobile handsets and base stations (Kim et al., 2004). In addition, reduction in signal loss, low power consumption, scaling down device size, reduction in materials and fabrication costs, and packaging of the device are main issues today. Some of these issues can be resolved, if the new generation of electroacoustic devices can be monolithically integrated with integrated circuit (IC). Conventional electroacoustic devices, used in the communication e.g. Surface Acoustic Wave (SAW) and Bulk Acoustic Wave (BAW) based systems, are widely used for today's wireless communication. These devices are typically made on a single crystal piezoelectric substrate such as quartz, lithium niobate, and lithium tantalate (Assouar et al., 2004). Unfortunately, these substrates based electroacoustic devices are made separately and then it is wired with the signal processing chip, which has several limitations, in particular low acoustic wave velocity and high frequency device fabrication. To resolve these two core issues, thin film materials based electroacoustic devices are actively under consideration [Bender et al., 2003]. Where, a crystalline film is grown on a particular substrate, especially silicon wafer and electroacoustic device is made out of crystalline film. Thus, the electroacoustic device can be integrated with the signal processing circuit. Apart from the silicon wafer as a base material for crystalline film deposition, a variety of other substrates are also explored for academic and technology interests. Furthermore, to get electroacoustic devices of better quality in terms of high frequency and high quality factor (Q), the piezoelectric property of the film is also exploited with different type of device concept called "Micro-Electro-Mechanical Systems" (MEMS). Thin film bulk acoustic resonators (TFBAR) comes under this MEMS devices, where the crystalline film is made to resonate at RF frequency. These MEMS

devices have smaller size, lower insertion loss and higher-power handling capabilities than conventional SAW devices (Lee et al., 2004).

Generally, thin piezoelectric films, such as aluminum nitride (AlN), zinc oxide (ZnO) and lead zirconium titanate (PZT) are used for high frequency acoustic devices (Loebl et al., 2003; Yamada et al., 2004; Schreiter et al. 2004). AlN has higher SAW velocity, lower propagation loss, and higher thermal stability in comparison to ZnO; whereas, PZT thin films need selective substrates for deposition and thereafter, needs post-deposition poling to get specific crystal orientation. Thus, AlN seems to have edge over the ZnO and PZT films for electroacoustic devices. The critical factor of piezoelectric AlN thin film is its crystal orientation and morphology. Furthermore, to integrate with the signal processing chip, it is also essential that AlN film should be compatible to the complementary metal oxide semiconductor (CMOS) fabrication processes. In addition, AlN being a dielectric material, it can be used as an insulating material in integrated circuits as well as a piezoelectric material in electroacoustic device. Thus, it is imperative to study the presence of electrical charges and the nature of generation of defects in the AlN film along with its morphology. Usually, there are four types of electric charges present in the insulating film; namely, bulk charges (Q_{in}) and interface (D_{it}) charges, fixed charges (Q) and mobile charges (Q_m). In present IC processing, the presence of fixed charges (Q) and mobile charges (Q_m) are eliminated upto a large extent. Furthermore, the bulk charges (Q_{in}) and interface (D_{it}) charges are reduced further by the optimization of growth parameter and the post-deposition treatments. Reduction in the bulk charge (Q_{in}) and interface charge (D_{it}) density is most essential in cantilever beam based MEMS resonator, otherwise the electrostatic force produced by the these charges may stuck cantilever beam on the substrate (Luo et al., 2006). Most of the MEMS are made out of single crystal silicon substrate utilizing well-matured IC fabrication technology. This poses a challenge to be compatible with a new generation of functional materials. Apart from the electrical charges, the selective etching of piezoelectric materials and silicon for electroacoustic device fabrication is a key technology.

2. Properties of AlN film

AlN is a III-V family compound having hexagonal wurtzite crystal structure with lattice constants $a = 3.112 \text{ \AA}$ and $c = 4.982 \text{ \AA}$ (Yim et al., 1973). In this structure, each Al atom is surrounded by four N atoms, forming a distorted tetrahedron with three Al---N_(i) ($i = 1, 2, 3$) bonds named B₁ and one Al---N₀ bond in the direction of the c-axis, named B₂. The bond lengths of B₁ and B₂ are 1.885 \AA and 1.917 \AA , respectively. The bond angle N₀---Al---N_i is 107.7° and that for N₁---Al---N₂ is 110.5° (Xu et al., 2001).

AlN has gained ground in semiconductor industry because of its unique electrical, mechanical, piezoelectric and other properties (Table 1). Some of these noteworthy properties are wide bandgap, high thermal conductivity, high SAW velocity, moderately high electromechanical coupling coefficient, high temperature stability, chemical stability to atmospheric gases below 700°C , high resistivity, low coefficient of thermal expansion (close to Si), high dielectric constant and mechanical hardness (Xu et al., 2001; Strite et al., 1992; Wang et al., 1994). Its high thermal conductivity (about 100 times that of SiO₂ and roughly equal to that of silicon) and electrical insulating property can prove to be a good dielectric layer for a new generation of integrated circuit devices, particularly in metal insulator semiconductor (MIS) devices. High heat dissipation of AlN can significantly enhance device lifetime and efficiency. AlN film with (002) preferred orientation (c-axis) has maximum

piezoelectricity among all other orientations of its crystal structure (Naik et al., 1999). Furthermore, its lattice matching is near to that of silicon and thus less stress is expected to be generated at the AlN/silicon interface. Owing to these properties, AlN films have received great interest as an electronic material for thermal dissipation, dielectric and passivation layers for ICs, acoustic devices, resonators and optoelectronic devices.

Bandgap	6.2 eV, direct
Thermal conductivity	2.85 Wcm ⁻¹ K ⁻¹
Coefficient of thermal expansion	4-5×10 ⁻⁶ K ⁻¹
Refractive index	1.8-2.2
Dielectric constant	8.5
Electrical resistivity	10 ¹¹ -10 ¹³ Ω.cm
SAW velocity	6000 m/sec
Melting point	2490 °C
Hardness	9 Mhos

Table 1. Properties of AlN

3. Synthesis of AlN film

Depending on the intended application, various techniques have been implemented for synthesizing AlN films; namely, molecular beam epitaxy (MBE), reactive evaporation, pulsed laser deposition (PLD), chemical vapour deposition (CVD) and sputtering. Among these techniques, sputtering has the advantage of low-temperature deposition, ease of synthesis, less expensive, non-toxic, good quality films with a fairly smooth surface [Kar et al., 2006; Kar et al., 2007]. In addition, sputtering technique has also CMOS process compatibility. In sputtering technique, plasma is created between the two electrodes by applying high voltage in low pressure. The plasma region contains, positive ions, electrons and neutral sputtering gas, thus the plasma behaves like a conducting medium. Usually, argon gas is used as a sputtering gas. The material that is to be sputtered is called target and it is fixed to the negatively charged electrode. The other electrode is called anode, which is grounded so that the ratio of the target to anode area is significantly reduced. This electric configuration of the sputtering system makes high electric field at the target and that enhances the rate of sputtering. During sputtering process, the energetic ions strike the target and dislodge (sputter) the target atoms. These dislodged atoms travel through the plasma in a vapour state and stick to the surface of wafers, where they condense and form the film. AlN film can be deposited either by directly using the AlN target or by sputtering of aluminum metal in presence of argon and nitrogen gas. The sputtered aluminum atoms react with the nitrogen gas and form AlN film. This process of film deposition is called "reactive sputtering deposition". The sputtering parameters are required to be optimized for desired morphological and electrical properties. These deposition parameters are mainly sputtering pressure, wafer to target distance, sputtering power and wafer temperature. AlN film deposition by reactive sputter deposition technique requires nitrogen as a reactive gas,

where it is introduced into the sputtering chamber along with inert argon gas. Argon ions produced in the plasma due to sputtering power and thereafter they strike to the aluminum target and sputter aluminum atoms. These aluminum atoms react with nitrogen and form AlN compound and that deposit on the wafer. Hence, the gas flow ratios need to be optimized. To increase sputtering rate, magnets are placed under the aluminum target, so that magnetic field and the electric field are perpendicular to each other. This configuration of sputtering system is called “magnetron sputtering technique”. In the magnetron sputtering, electrons travel in spiral motion in the plasma region. This increases the collision of electrons to neutral argon atoms significantly and that increases argon ions in many folds, thus sputtering rate becomes high.

AlN film can be deposited by DC (direct current) and RF (radio frequency, 13.56 MHz) magnetron sputtering modes. In the DC mode of sputter deposition, the target material must be conductive, so that plasma can sustain. If trace of impurity is present in the system, the surface of the aluminum target becomes contaminated and target poisoning takes place. On the other hand, RF sputtering has the major advantages to produce good quality film, high deposition rate and less chance of target poisoning. For these reasons, RF sputtering technique is preferred than the DC sputtering technique. To obtain well oriented crystalline AlN films for SAW and MEMS structures, the RF sputtering parameters need to be optimized. The sputtering parameters are: RF power, substrate temperature, sputtering pressure, nitrogen concentration and target-substrate distances (D_{ts}). AlN films are deposited on CMOS IC compatibility silicon (100) wafer by the RF reactive magnetron sputtering. The change in morphological and electrical properties of the AlN films with the growth parameters are reported in following section.

3.1 RF power

Amorphous AlN film is found at lower RF sputtering power (100 W), but films became (002) oriented at a sputtering power of 200 W. Further increase of RF power to 400 W, a significant increase in (002) orientation has taken place. This is due to the increase of kinetic energy of atoms that leads to atomic movements on the substrate surface as a result of higher RF power. These newly arrived surface atoms are called “ad-atom”. Higher sputtering power increases the AlN grain size that leads to increase in surface roughness as shown in scanning electron microscope (SEM) images (Fig. 1) (Kar et al., 2009).

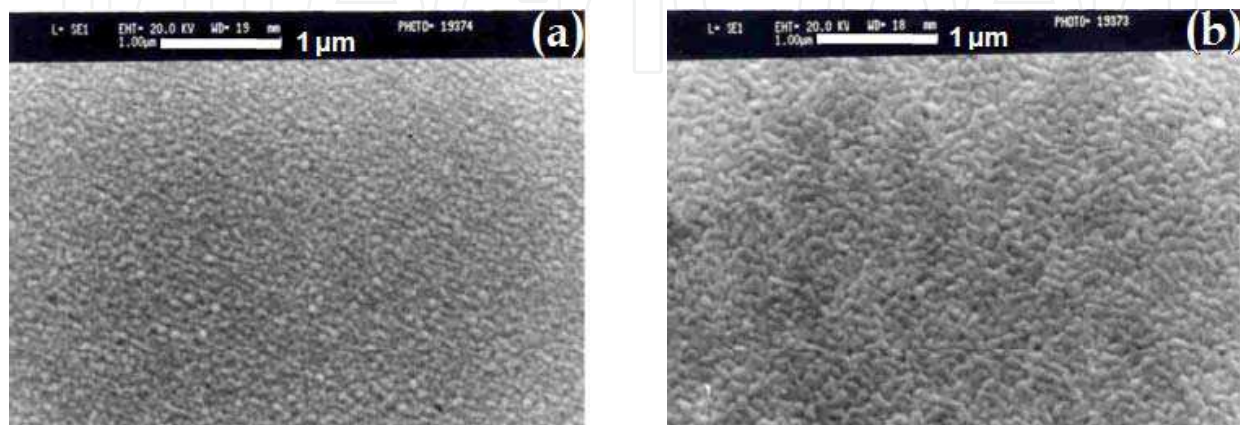


Fig. 1. SEM micrographs of AlN films deposited at (a) 200 W, and (b) 300 W

3.2 Substrate temperature

The structural and morphological properties of the deposited AlN films are strongly dependent on the kinetics of the sputtered atoms arrived at the substrate. The kinetics of sputtered atoms depends on the sputtering parameters. For instance, substrate temperature increases the ad-atom mobility and changes the film morphology significantly. One such illustrations of morphological change with temperature are seen from the X-Ray diffraction (XRD) studies. It is clearly seen from the XRD studies that the *c*-axis oriented AlN (002) peaks become prominent at moderate temperature range (200–300 °C), but degrades significantly at 400 °C (Kar et al., 2006). This can be attributed to the structural disorderness resulting from the incorporation of impurity atoms at higher temperature (Wang, 2000). The amount of contamination depends on the sputtering deposition system and process related factors, such as base pressure, temperature, gas purity and the partial pressure of moisture, etc. (Naik et al., 1999). Furthermore, smaller grain size with smoother surfaces is observed at lower deposition temperature, and that increases with temperature (Fig. 2). A possible reason may be that the smaller grains grow and merge to form bigger grain, due to the higher thermal energy.

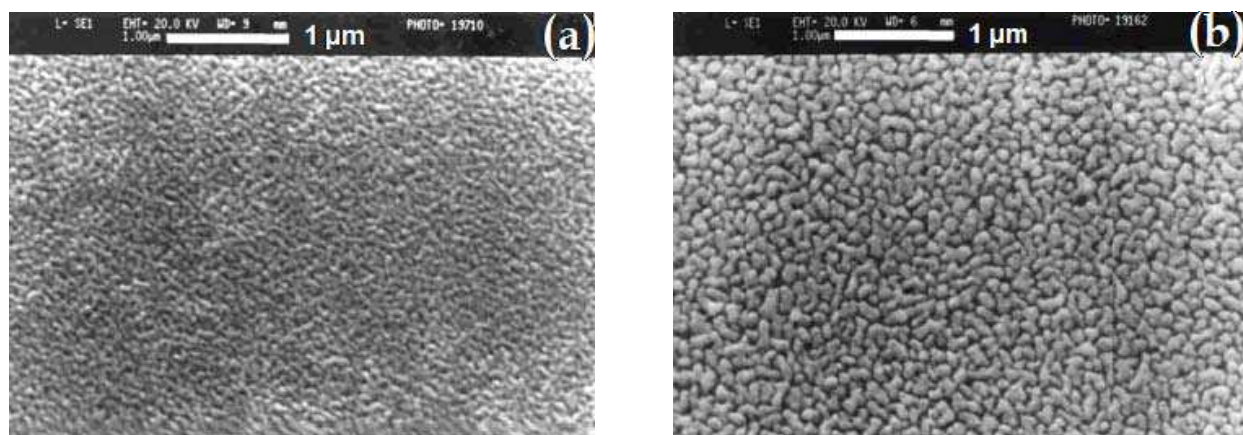


Fig. 2. SEM micrograph of AlN films deposited at (a) 100 °C, and (b) 400 °C

3.3 Sputtering pressure

The variation in crystal orientation with different sputtering pressure are observed from the XRD studies, where the intensity of (002) orientation increases with the deposition pressure and attained a maximum value at 6×10^{-3} mbar. On further increase to a deposition pressure of 8×10^{-3} mbar, the (002) crystal orientation of the AlN film is changed abruptly to the (100) orientation with lesser intensity. The deposited atoms may have altered their direction, energy, momentum and mobility due to the decrease in mean free path of the atoms with sputtering pressure. The hexagonal wurtzite structure of AlN has two kinds of Al–N bond named as B_1 and B_2 . These bonds B_1 and B_2 together correspond to (110) and (002) planes, where B_1 corresponds to (100) plane. The formation energy of B_2 is relatively larger than that of B_1 (Cheng et al., 2003). Hence, the energy required for sputtering species to orient along *c*-axis is larger than the other possible planes. At low pressure, sputtering species possess enough energy to form hexagonal wurtzite crystalline structure on substrate surface. It is also reported that the surface roughness of the film increases with the increase in deposition pressure. The grain size is increased till 6×10^{-3} mbar deposition pressure and then it reduced to 80 nm at 8×10^{-3} mbar (Kar et al., 2006). In addition, inhomogeneous patterns on the surface are also observed at this higher pressure (Fig. 3). It is also observed that the AlN film

has changed its orientation with less Al-N bond density and reduction of grain size at 8×10^{-3} mbar sputtering pressure. Hence, it is inferred that the structural disorder and/or the change in the Al-N bond density/angles must have taken place at this particular sputtering pressure.

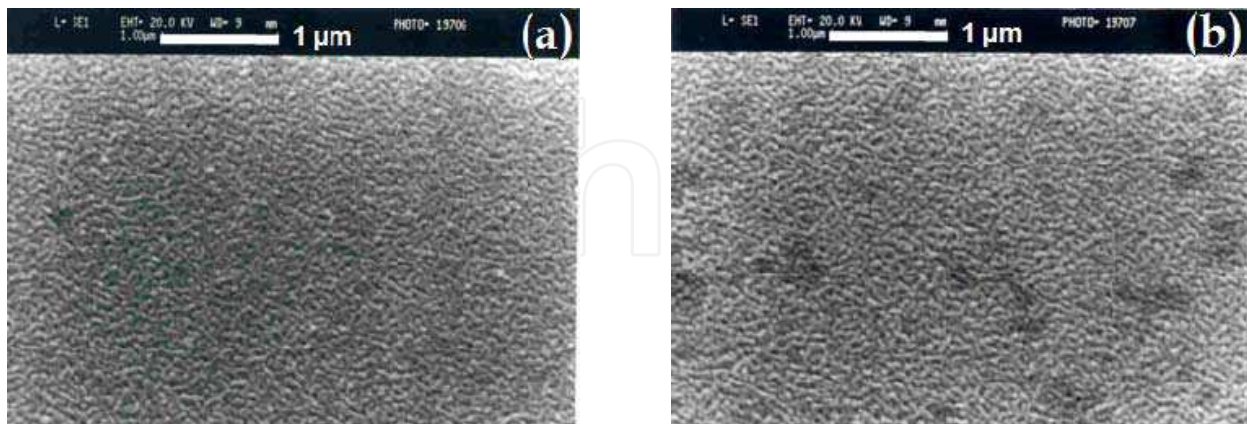


Fig. 3. SEM micrograph of the AlN films deposited at (a) 2×10^{-3} mbar, and (b) 8×10^{-3} mbar

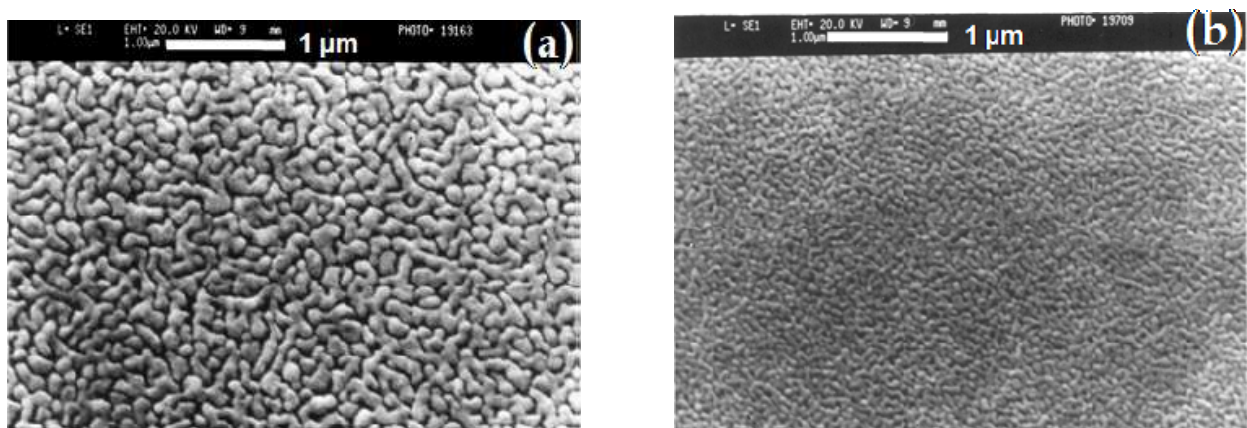


Fig. 4. SEM micrograph of AlN films deposited at (a) 20 % N_2 , and (b) SEM image of AlN film for D_{ts} of 5 cm

3.4 Gas flow ratio

At lower nitrogen concentration, the intensity of (100) peak is relatively more prominent than (002), but the trend reverses with higher nitrogen concentration (Kar et al., 2006). At 80% N_2 , a highly oriented (002) peak is observed without trace of (100) orientation. Lower argon and higher nitrogen gas concentration results slower aluminum sputtering rate. If the time interval for the arrival of Al species at the wafer surface is slower, the Al atom gets enough time to react with N_2 . This increases the probability of Al-N bond formation and bonded Al-N molecules get more time to adjust themselves along (002) orientation on the substrate. On the other hand, at higher argon concentration, Al does not get enough time for complete nitridation due to higher sputtering rate. In addition, faster arrival of the Al at the substrate surface results not only in a poor AlN bond, but also provides less time for the newly formed AlN to arrange itself along c-axis. A surface texture of smaller grain size, smoother, homogeneous and dense granular microstructures has been observed at higher concentrations of nitrogen. This indicates a low surface mobility of the ad-atoms at high

nitrogen concentration. In contrast, bigger grain size with increased roughness is observed at lower nitrogen concentration, where the newly formed smaller grain merges together with a previously formed grain and becomes bigger in size. The size and distribution of the micrograins is quite uniform at 80% nitrogen concentration. At lower nitrogen concentrations, Ar⁺ ions transfer more energy to the Al target during bombardment, generating more aluminum atoms that make clusters with incomplete nitridation of aluminum on the wafer surface. This leads to formation of fewer bonds, a poor c-axis orientated and a rough film (Fig 4 (a)).

3.5 Target-substrate distance

The kinetics of the sputtered species arriving at the substrate controls the ad-atom mobility and atomic rearrangement that governs the microstructure of the film. From the XRD studies, it is observed that the intensity of c-axis orientation of the film decreases with increase in target to substrate distance D_{ts} (Kar et al., 2008). At shorter D_{ts} , the Ar ions travel almost normal to the target due to the high electrical field and knock out Al atoms around perpendicular to the target. Because of short deposition path, the probability of collisions of the Al atom with gas atoms is low. Therefore, a good quality film is obtained at lower D_{ts} (5 cm). On the other hand, at larger D_{ts} , the chances of Al collision with gas molecules is increased. In this process Al atoms lose its kinetic energy significantly as well as alter deposition angles. These randomly arriving Al atoms, with lesser energy, cause self-shadowing effects and reduce atomic migration that leads to generation of voids in the film (Lee et al., 2003). The grain size of the AlN film increases with D_{ts} . For lower D_{ts} , smaller grain with minimum surface roughness is observed (Fig. 4(b)) and a coarser grain is found at the highest D_{ts} (8 cm). Surface roughness of the synthesized AlN films are also increases with D_{ts} . The kinetic energy of deposited species is considered to be a major factor for the grain size and the surface roughness of the film.

3.6 Variation of electrical properties with sputtering parameter

The AlN film can be used as a dielectric layer in IC; hence, the electric charges are essential to study with the sputter deposition parameters. Electric charges like Q_{in} and D_{it} are highly governed by the sputter deposition parameters. A decrease in the Q_{in} is observed with sputtering power, where as D_{it} is found to be minimum at moderate RF power. At higher temperature, better electrical properties in the bulk as well as the interface of sputtered AlN films are reported; this is mainly due to the formation of bigger grain size and its associated effects. It is reported that the defects produced by stress, voids and incorporation of gases are main responsible cause for the monotonic increase in Q_{in} . The D_{it} has a minimum value at 6×10^{-3} mbar sputtering pressure. The Q_{in} and D_{it} increases with nitrogen concentration. This will have a deleterious effect for silicon-based devices at higher nitrogen concentration. Rise in the Q_{in} and D_{it} with the increase in D_{ts} is also reported. It is seen that at larger D_{ts} , the morphological as well as the electrical properties of the AlN films deteriorates, whereas, at shorter D_{ts} the quality of the film comes out to be better (Kar et al., 2007). Apart from the electric charges, it is observed that better crystallinity posses AlN films of higher dielectric constant.

4. Post-deposition annealing effect

AlN film may see high temperature, if AlN film is monolithically integrated during IC fabrication. Post-deposition heat treatment significantly affects the morphology and electric

charges of AlN film. The post-deposition thermal treatments (annealing) of AlN film are generally carried out by two distinguished modes; namely, Rapid Thermal Annealing (RTA) and conventional furnace annealing.

4.1 Rapid thermal annealing (RTA) process

The XRD studies show that the intensity of c-axis (002) orientation increases upto annealing temperature of 800 °C in nitrogen ambient and then it marginally decreases at 1000 °C (Kar et al., 2005). The shift in XRD diffraction peaks is reported at higher temperatures, which may be due to the generation of stress. Granular worm-like nanostructures are found in as-deposited AlN films (Fig. 5), whereas cracks are observed for annealing at 1000 °C. A short duration of heat pulse by RTA is barely sufficient to modulate the film surface, but not enough to activate the grains of the AlN films to merge themselves to form bigger grains. Appearances of cracks are due to the stress developed in the film. The thermal coefficient mismatch between the AlN and silicon substrate may be generated from the fast ramp up and ramp down annealing heat cycle during rapid thermal annealing. The position and density of cracks depend strongly on the defects, dislocations and the structural relaxation of grain boundaries. The surface roughness is considerably increased for the film annealed at higher temperatures due to the surface modulation.

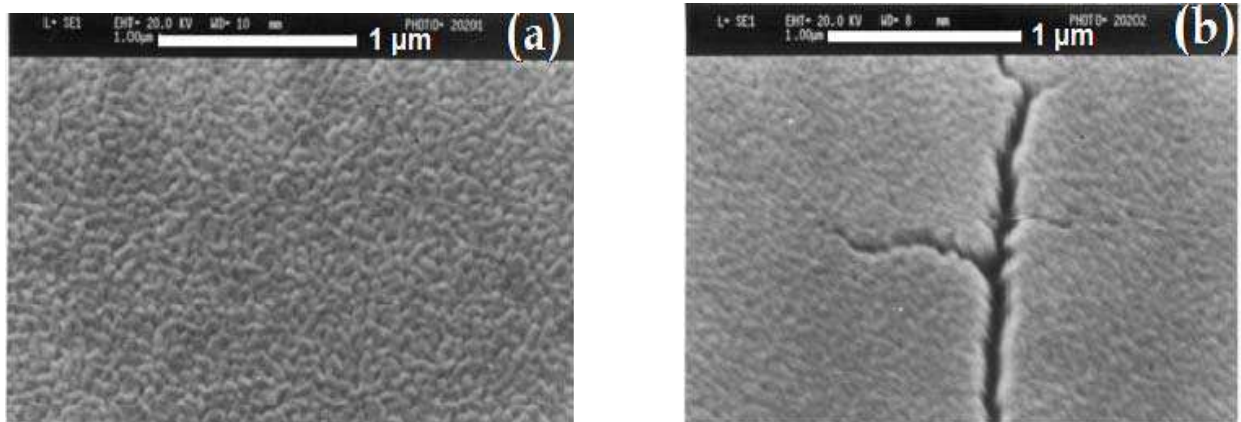


Fig. 5. SEM micrograph of AlN films RTA processed at (a) as-deposited, and (b) 1000 °C

4.2 Furnace annealing

The intensity of the (002) peak increases with furnace annealing temperature, where the atoms acquire adequate activation energy to become (002) oriented. Sometimes, many of the atoms may not be at the crystal lattice site in the as-deposited AlN film, which causes the lattice strain and the formation of microvoids. During conventional furnace annealing, atoms get enough time to acquire sufficient kinetic energy and occupy relative equilibrium positions that minimize the lattice strain and microvoids, which results in a better crystalline film. Furthermore, the furnace annealing process minimizes the dislocations and the other structural defects and forms a better stoichiometric material. From the SEM micrographs, it is observed that the granular worm-like textures grow bigger in size with increased surface roughness as a result of annealing (Fig. 6). The possible reasons for increase in the grain size and the surface roughness may be due to atomic migration in the film towards the lower surface energy with annealing temperature (Kar et al., 2009).

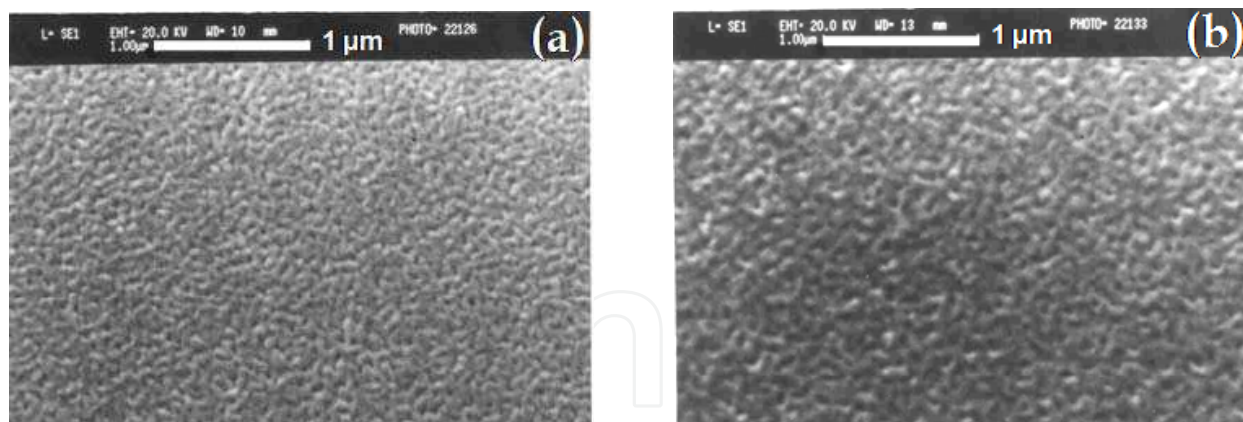


Fig. 6. SEM micrograph of AlN films annealed at (a) as-deposited, and (b) 800 °C

4.3 Effect of annealing on electrical properties

In both types of annealing, the Q_{in} is increased with temperature. The probable reasons for the rise in the Q_{in} may be due to the generation of trap centres with annealing in the nitrogen ambient. In RTA, the D_{it} is found to be strongly dependent on the annealing temperature and it significantly reduced at 600°C. With furnace annealing, the D_{it} decreases with increase in annealing temperature.

5. Growth of AlN films on different substrates

Many a times, AlN films are made on an insulator (SiO_2) for isolation or it is deposited over the metallic electrodes for thin film resonators (TFR). In future, AlN film on high speed semiconductor substrates such as GaAs, InP can be exploited for high speed signal processing and Micro-Opto-Electro-Mechanical Systems (MOEMS) applications. Hence, integration of AlN films on GaAs and InP substrates for a new generation of high-speed devices/subsystems, especially for telecommunications, and radar applications are required. Growth and surface morphology of a deposited film depends not only on the kinetics of the arriving species at the substrate, but also on the nature of the substrates chosen, even if they belong to the same family. In addition, substrate orientation, thermal conductivity and thermal expansion coefficients play vital roles in film growth and its morphology. C-axis oriented AlN films are deposited on Si and SiO_2/Si substrates by RF reactive magnetron sputtering, where the degree of orientation decreases with increase in oxide thickness. The surface roughness of the films deposited on SiO_2/Si is higher. AlN films are also deposited on GaAs and InP substrates by reactive magnetron sputtering technique under identical deposition conditions. c-axis (002) oriented films are observed on GaAs substrates; whereas, AlN (100), (002) and (102) oriented peaks are seen in case of InP substrates. Surface morphology of the films deposited on Si and InP substrates seems to be similar, but the films on InP are little rougher with the development of nano-pores. AlN films, grown on GaAs substrates, forms bump like structures (Kar et al., 2009), which may be due to thermal and/or lattice mismatch. It is important to note that the crystallinity and stoichiometry of the initial layer of AlN film also plays a significant role in the creation of defects and mismatches (Ahmed et al., 1992). Crystal orientation of AlN films is also a strong function of the bottom metal electrodes. AlN films deposited on metals (Al, Cu, Cr, Au) are c-axis oriented, whereas the films deposited on Al and Cu are rough with larger grains.

6. AIN film based acoustic device

SAW and BAW are two important types of acoustic wave devices used in RF communication. These devices can be realized either on a solid substrate/film or through micromachined suspended beam structures. In SAW devices, an elastic wave travels on the surface of a piezoelectric material and displaces the atoms about their equilibrium positions at the interface of piezoelectric film and solid substrate. The neighboring atoms at the interface then produce restoring forces to bring the displaced atoms back to their original positions. SAW can be generated by placing two inter digital transducers (IDT) either sides of the substrate. These IDTs have alternating periodic fingers (Fig. 7). RF signal is applied one of these alternating polarity fingers (IDT) that produces elastic mechanical wave in the substrate. This wave travels along the substrate and also collected by placing another IDT on the piezoelectric material, some distance away from the first IDT. The second IDT collects the RF signal, which can be retransformed into the electric signal. As the elastic-mechanical wave has the speed of acoustic wave, it introduces the delay of signal by 10^3 order. This is the prime use of SAW device. The periodicity p , (centre-to-centre spacing between neighbouring IDT fingers of same polarity) becomes the wavelength of the acoustic wave, and dictates its frequency $f = v/p$, where f and v represent acoustic wave frequency and acoustic propagation velocity, respectively.

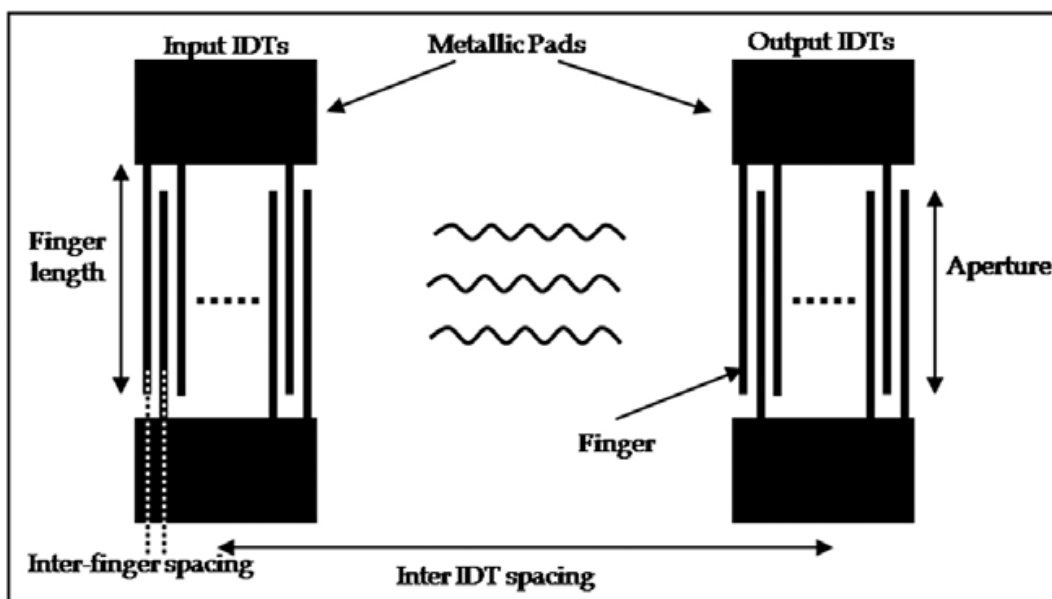


Fig. 7. Schematic diagram of SAW device

Thin Film Bulk Acoustic Resonator (FBAR) device consisting of a piezoelectric material sandwiched between two electrodes and is acoustically de-coupled from the surrounding medium. FBAR devices, using AlN piezoelectric with thickness ranging from tenth of micrometers to several micrometers, resonate in the cellular bands of cell phones and other wireless applications. On applying voltage across the electrodes, the piezoelectric thin film undergoes a shear deformation, and a BAW resonance occurs in the AlN film due to coherent reflection at the top and bottom boundaries of the metal film or plate electrodes. The frequency of resonance is dependent on the physical structures; hence, desired resonant frequency can be obtained by tailoring physical dimension of the structure. For RF frequency, physical dimension of resonators can be realized by using MEMS technology.

MEMS resonators are comprised of a microscale mechanical element, which converts mechanical to electrical signal and vice versa. One of the prominent resonator structures is MEMS cantilever, which is based on thin piezoelectric films. Film resonates when an ac voltage is applied across the film. Resonator can be made without piezoelectric material (electrostatic, capacitive resonator), but it suffers with large resistance, in the range of $M\Omega$, and depends on driving voltage. On the other hand, piezoelectric resonators have smaller resistance of the order of $K\Omega$ and are more suitable for UHF device applications. (Lakin, 1999; Quandt et al., 2000; Humad et al., 2003). In addition, the output is easier to sense in a piezoelectric resonator. Furthermore, a piezoelectric resonator has certain advantages over the electrostatic resonator (capacitive resonators), such as low current consumption and lower actuation voltages (Olivares et al.; 2005). But the quality factor (Q) of piezoelectric resonator is smaller than that of a capacitive resonator. The quality factor of any resonator is proportional to the decay time, and is inversely proportional to the bandwidth around resonance. Higher Q represents higher frequency stability and accuracy capability of the resonator (De Los Santos, 1999).

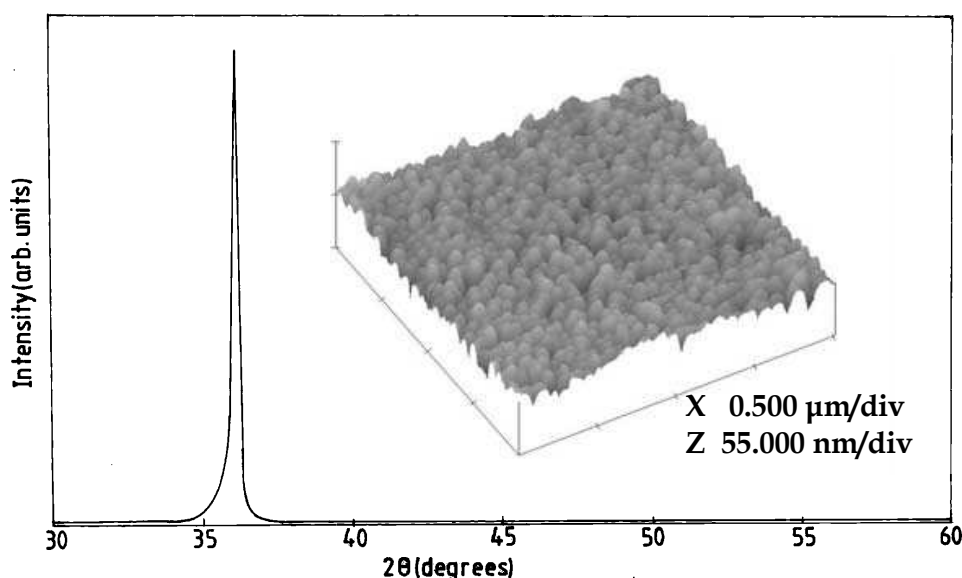


Fig. 8. XRD pattern, and AFM image (inset) of sputtered AlN film for SAW

6.1 Evaluation of AlN films through SAW devices

Higher RF power (400 W) and nitrogen concentration (80%), moderate substrate temperature (200 °C) and sputtering pressure (6×10^{-3} mbar), lower target-substrate distance (5 cm) is suitable for the growth of smooth, highly c-axis oriented AlN film with better electrical properties. A c-axis (002) oriented peak is recorded at 2θ value of 36.1° (Fig. 8). The atomic force micrograph of the film shows dense microstructure with continuous grain growth (inset of Fig. 8). This kind of film is suitable for SAW devices. In a typical case, each IDT consisted of 25 pairs of fingers/electrodes with $30 \mu\text{m}$ centre-to-centre spacing between the two neighbouring fingers comprising a pair ($p/2$). The width of each finger/electrode is designed to be $15 \mu\text{m}$ ($p/4$) with each of 6.0 mm length and 5.0 mm overlap, producing a SAW filter with an acoustic wavelength of $60 \mu\text{m}$ (Kar et al., 2009). The SAW device parameters are: AlN film thickness = $0.92 \mu\text{m}$, acoustic wavelength = $60 \mu\text{m}$, SAW velocity = 5058 m/sec, electromechanical coupling coefficient (K^2) = 0.34%.

Time response, due to acoustic frequency alone, is found after the gating out the response due to electromagnetic feed through. For the centre to centre distance between the two IDT's (d) = 7 mm, the main SAW signal centred at time (delay) = $d / V_{\text{SAW}} = 7 / 5058 = 1.384 \mu\text{s}$ is obtained. The central acoustic frequency (f_0) response after the gating out is observed at 84.304 MHz (Fig. 9).

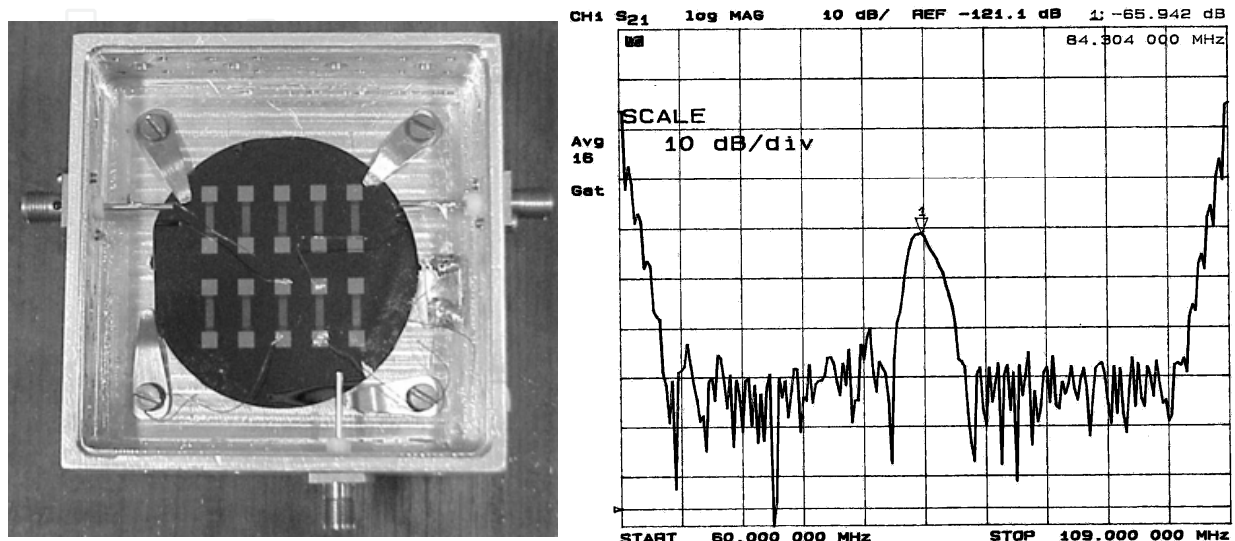


Fig. 9. (a) Optical image of AlN based SAW devices, and (b) Measured response of the SAW device

6.2 Fabrication of AlN film based MEMS

Anisotropic etching of silicon is a key technology for fabrication of various three-dimensional structures such as thin membranes and microbridges for MEMS. Generally, anisotropic silicon etching is done by potassium hydroxide (KOH) or ethylenediamine pyrochatechol (EDP) etchant (French, 2001; Ni et al., 2005). Another technique, which is more versatile, CMOS process compatible and nontoxic, provides better selective etching using doped tetramethylammonium hydroxide (TMAH) etchant (Biswas et al., 2006). The characteristics of these three etchants are listed in Table 2. Many AlN and Al based MEMS structures are also isolated from silicon by silicon dioxide. Hence, their selective etching is very important. Diluted tetramethylammonium hydroxide (TMAH, 5 wt %), doped with silicic acid (30.5 g/l) and ammonium persulphate (5.5 g/l), is suitable for CMOS silicon microprocessing. To protect Al and AlN, silicic acid has been chosen instead of pure silicon powder, because silicic acid dissolves quickly in TMAH solution. Ammonium persulphate (AP) is also added to the above-mentioned solution to reduce the surface roughness of etched silicon. The etch rate of silicon in doped TMAH is found to be 50 $\mu\text{m}/\text{hour}$. During silicon etching the Al, AlN and SiO_2 films are used as mask layers (Fig. 10). Low etch rates of Al and AlN (18-30 nm/hour) as well as SiO_2 (2.5 nm/hour) are found to be suitable for MEMS applications. Probable reason for low etch rate of Al may be the formation of a passivating layer during TMAH etching (Fujitsuka et al., 2004). Dilute TMAH is a well known etchant for AlN film (Kim et al., 2004) and Al as well. But doped TMAH shows significantly lower etch rates for AlN and Al, which are exploited for AlN based suspended microstructures. Fig. 10 (d) depicts suspended Cr/AlN/Cr/ SiO_2 cantilevers fixed at one end, where in one of the microstructures is lifted up because of the stress (Kar et al., 2009).

Property	KOH	EDP	TMAH
Si etch rate (100), $\mu\text{m}/\text{h}$	150	30-35	40-60
Etch quality	high	high	medium
Selectivity (111)/(100)	1:30-100	1:20	1:10-50
Under-etch rate	0.5-1.5	1.4-1.5	0.2-1.7
CMOS compatible	no	yes	yes
Selectivity PECVD SiO_2/Si	1:100-300	1:10,000	1:100-1000
Selectivity PECVD SiN/Si	1:10,000	-----	1:150-200
Attack of aluminum	high	medium	low with Si
Etch stop	boron dope	boron dope	boron dope
Toxicity	low	high	low
Long-term stability	high	low	medium
Cost	low	high	medium

Table 2. Characteristics of important wet etchants used for silicon micromachining (French, 2001)

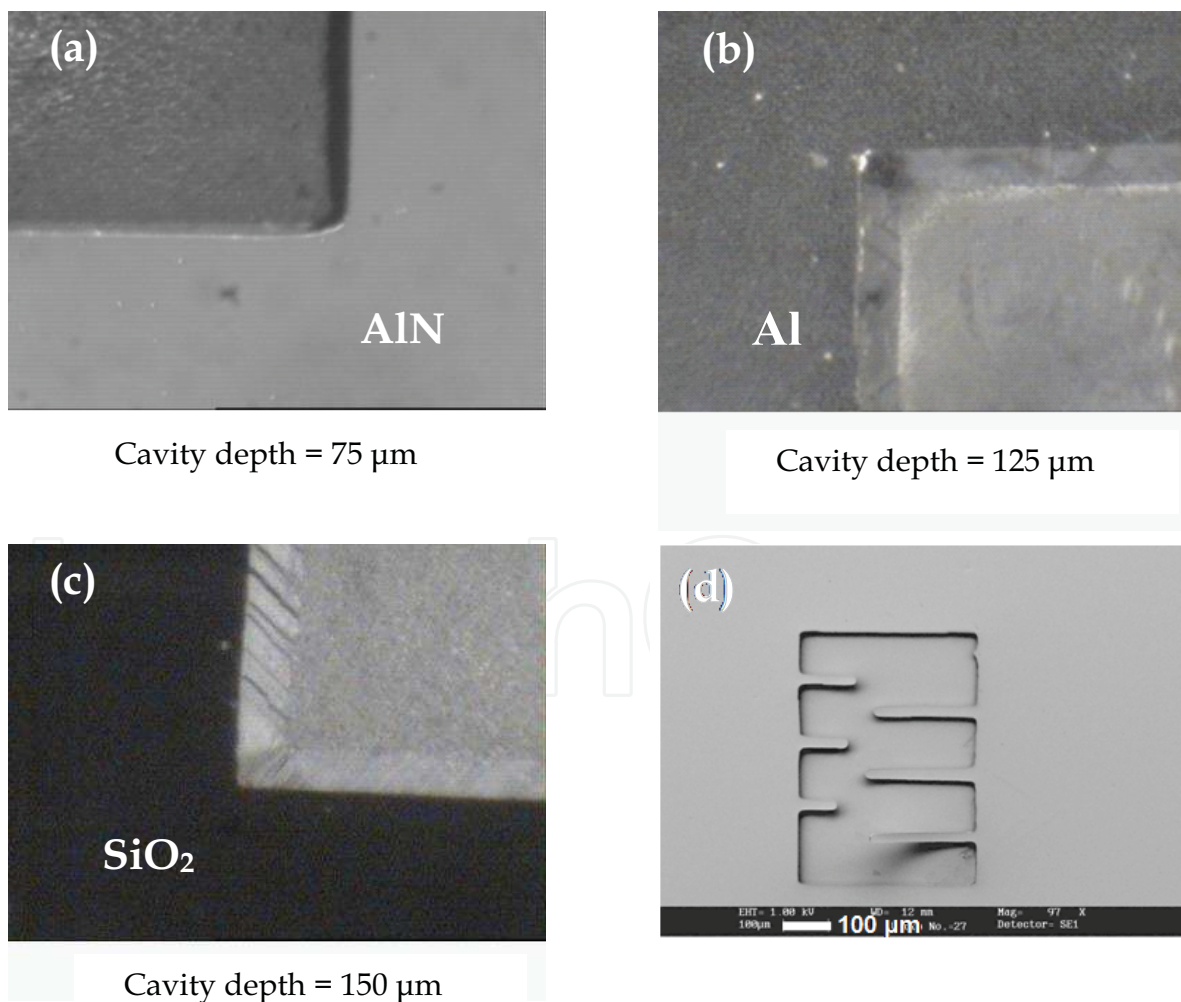


Fig. 10. Micrographs of etched silicon (a) AlN/Si, (b) Al/Si, (c) SiO_2/Si , (d) AlN based suspended microstructures

7. Conclusion

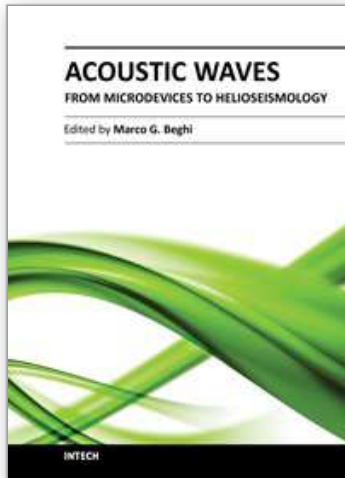
This chapter focuses on the study of RF sputtered AlN films in view of ICs, acoustic devices and MEMS applications. It is divided into two distinct parts; growth, characterization and optimization of device worthy AlN film (mostly on silicon), and demonstration of acoustic and MEMS device applications. The morphological and electrical properties of RF sputtered AlN films are studied with sputtering power, deposition temperature, sputtering pressure, gas flow ratio and target to substrate spacing (D_{ts}). Higher RF power (400 W) and nitrogen concentration (80%), moderate substrate temperature (200 °C) and sputtering pressure (6×10^{-3} mbar), lower target-substrate distance (5 cm) is suitable for the growth of smooth, highly c-axis oriented film with better electrical properties. Post-deposition (RTA and furnace) annealing has a significant impact on the morphology as well as the electrical properties. The RTA processed AlN films have relatively high c-axis (002) orientation films at 800 °C, where microcracks are appeared during RTA process at 1000 °C. Bulk charge density is increased with annealing temperature both types of annealing. A significant reduction in interface charge density is found at 600°C with RTA process, whereas it decreases with furnace annealing temperature. AlN films are deposited and characterized on different substrates by RF reactive magnetron sputtering. On SiO₂/Si substrates, (002) orientation is deteriorated and surface roughness of the films is increased with the increase in oxide thickness. c-axis (002) oriented films are observed on Si and GaAs substrates, whereas AlN (100), (002) and (102) oriented peaks are seen on InP substrates. AlN films, deposited on GaAs substrate, show bump like structures. c-axis oriented AlN films are also observed on metallic films. The AlN films, deposited on Al and Cu, are found to be rough with larger grains. Piezoelectric nature of RF deposited AlN films is ascertained from the performance of a SAW device. This device is centred around a frequency of 84.3 MHz and acoustic phase velocity is inferred to be 5058 m/ sec with K^2 of 0.34 %. The TMAH solution, doped with an appropriate ratio of silicic acid and ammonium persulphate, is developed for micromachining of AlN based structures. The etch rate of silicon is around 50 µm/hour. On the otherhand, the doped solution has negligible impact on Al, AlN and SiO₂ films. The growth of highly (002) oriented AlN films, post deposition process and micromachining method will provide an appropriate platform for the fabrication of futuristic electronic devices.

8. References

- Ahmed, A.U., Rys, A., Singh, N., Edgar, J.H. & Yu, Z.J. (1992). The Electrical and Compositional Properties of AlN-Si Interfaces, *J. Electrochem Soc*, Vol. 139(4), pp. 1146-1151.
- Assouar, M.B., Hakiki, M.E., Elmazria, O., Alnot, P. & Tiusan, C. (2004). Synthesis and microstructural characterisation of reactive RF magnetron sputtering AlN films for surface acoustic wave filters, *Diamond and Related Materials*, Vol. 13, pp. 1111-1115.
- Belyanin, A.F., Boulov, L.L., Zhirnov, V.V., Kamenev, A.I., Kovalskij, K.A. & Spitsyn, B.V. (1999). Application of aluminum nitride films for electronic devices, *Diamond and Related Materials*, Vol. 8, pp. 369-372.
- Bender, S., Dickert, F.L., Mokwa, W. & Pachatz, P. (2003). Investigations on temperature controlled monolithic integrated surface acoustic wave (SAW) gas sensors, *Sensors and Actuators B*, Vol. 93, pp. 164-168.

- Biswas, K., Das, S., Maurya, D. K., Kal, S. & Lahiri S.K. (2006). Bulk micromachining of silicon in TMAH-based etchants for aluminum passivation and smooth surface, *Microelectronics Journal*, Vol. 37(4), pp. 321-327.
- Cheng, H., Sun, Y. & Hing, P. (2003). The influence of deposition conditions on structure and morphology of aluminum nitride films deposited by radio frequency reactive sputtering, *Thin Solid Films*, Vol. 434, pp. 112-120.
- De Los Santos, H.J. (1999). Introduction to Microelectromechanical (MEM) Microwave Systems, Artech House, pp. 83.
- French, P.J. (2001). Integration of silicon MEMS devices: Materials and processing considerations, *Smart Materials Bulletin*, January, pp. 7-13.
- Fujitsuka, N., Hamaguchi, K., Funabashi, H., Kawasaki, E. & Fukada, T. (2004). Silicon anisotropic etching without attacking aluminum with Si and oxidizing agent dissolved in TMAH solution, *Sensors and Actuators A*, Vol. 114, pp. 510-515.
- Humad, S., Abdolvand, R., Ho, G.K. & Ayazi F. (2003). Micromechanical Piezo-on-Silicon Block Resonators, in *Proc. IEEE International Electron Devices Meeting (IEDM'03)*, Washington DC, Dec., pp. 957-960.
- Kar, J.P., Mukherjee, S., Bose, G., Tuli, S. & Myoung, J.M. (2009), Impact of post-deposition annealing on the surface, bulk and interface properties of RF sputtered AlN films, *Materials Science and Technology*, Vol. 25, pp. 1023-1027.
- Kar, J.P., Bose, G., Tuli, S., Myoung, J.M. & Mukherjee, S. (2009). Morphological investigation of AlN films on various substrates for MEMS applications, *Surface Engineering*, Vol. 25, pp. 526-530.
- Kar, J.P., Bose, G., Tuli, S., Dangwal, A. & Mukherjee, S. (2009). Growth of AlN films and its process development for the fabrication of acoustic devices and micromachined structures, *Journal of Materials Engineering and Performance*, Vol. 18, pp. 1046-1051.
- Kar, J.P., Mukherjee, S., Bose, G. & Tuli, S. (2008). Effect of inter-electrode spacing on structural and electrical properties of AlN films, *Journal of Materials Science: Materials in Electronics*, Vol. 19, pp. 261-265.
- Kar, J.P. (2007). *Growth and characterization of aluminum nitride (AlN) films for electroacoustic and MEMS applications*, Ph. D. thesis, Indian Institute of Technology Delhi, India
- Kar, J.P., Bose, G. & Tuli, S. (2006). A study on the interface and bulk charge density of AlN films with sputtering pressure, *Vacuum*, Vol. 81, pp. 494-498.
- Kar, J.P., Bose, G. & Tuli, S. (2006). Correlation of electrical and morphological properties of sputtered aluminum nitride films with deposition temperature, *Current Applied Physics*, Vol. 6, pp. 873-876.
- Kar, J.P., Bose, G. & Tuli, S. (2006). Influence of nitrogen concentration on grain growth, structural and electrical properties of sputtered aluminum nitride films, *Scripta Materialia*, Vol. 54, pp. 1755-1759.
- Kar, J.P., Bose, G. & Tuli, S. (2005). Influence of rapid thermal annealing on morphological and electrical properties of RF sputtered AlN films, *Materials Science in Semiconductor Processing*, Vol. 8, pp. 646-651.
- Kim, H.H., Ju, B.K., Lee, Y.H., Lee S.H., Lee J.K. & Kim, S.W. (2004). Fabrication of suspended thin film resonator for application of RF bandpass filter, *Microelectronics Reliability*, Vol. 44, pp. 237-243.
- Lakin, K. (1999). Thin film resonators and filters, *IEEE Ultrasonics Symposium*, pp. 895-906.

- Lee, H.C., Park, J.Y., Lee, K.H. & Bu, J.U. (2004). Preparation of highly textured Mo and AlN films using a Ti seed layer for integrated high-Q film bulk acoustic resonators, *J. Vac. Sci. Technol. B*, Vol. 22(3), pp. 1127-1133.
- Lee, S.H., Yoon, K.H., Cheong, D. S. & Lee, J.K. (2003). Relationship between residual stress and structural properties of AlN films deposited by r.f. reactive sputtering, *Thin Solid Films*, Vol. 435, pp. 193-198.
- Loebl, H.P., Klee, M., Metzmacher, C., Brand, W., Milsom, R. & Lok, P. (2003). Piezoelectric thin AlN films for bulk acoustic wave (BAW) resonators, *Materials Chemistry and Physics*, Vol. 79, pp. 143-146.
- Luo, J.K., Lin, M., Fu, Y.Q., Wang, L., Flewitt, A.J., Spearing, S.M., Fleck, N.A. & Milne, W.I. (2006). MEMS based digital variable capacitors with a high-*k* dielectric insulator, *Sensors and Actuators A*, Vol. 132 (1), pp. 139-146.
- Naik, R.S., Reif, R., Lutsky J.J. & Sodini, C.G. (1999). Low-Temperature Deposition of Highly Textured Aluminum Nitride by Direct Current Magnetron Sputtering for Applications in Thin-Film Resonators, *J. the Electrochemical Society*, Vol. 146(2), pp. 691-696.
- Ni, H., Lee H.J. & Ramirez, A.G. (2005). A robust two-step etching process for large-scale microfabricated SiO₂ and Si₃N₄ MEMS membranes, *Sensors and Actuators A*, Vol. 119, pp. 553-558.
- Olivares, J., Iborra E., Clement M., Vergara, L., Sangrador, J. & Sanz-Hervás, A. (2005). Piezoelectric actuation of microbridges using AlN, *Sensors and Actuators A*, Vol. 123-124, pp. 590-595.
- Quandt, E. & Ludwig, A. (2000). Magnetostrictive actuation in microsystems, *Sensors and Actuators A*, Vol. 81, pp. 275-280.
- Schreiter, M., Gabl, R., Pitzer, D., Primig, R. & Wersing, W. (2004). Electro-acoustic hysteresis behaviour of PZT thin film bulk acoustic resonators, *J. the European Ceramic Society*, Vol. 24, pp. 1589-1592.
- Strite, S. & Morko, H. (1992). GaN, AlN and InN: A review, *J. Vac. Sci. Technol. B*, Vol. 10(4), pp. 1237-1266.
- Wang, H.H. (2000). Properties and preparation of AlN thin films by reactive laser ablation with nitrogen discharge, *Modern Physics Letters B*, Vol. 14, 523-530.
- Wang, X.D., Jiang, W., Norton, M.G. & Hips, K.W. (1994). Morphology and orientation of nanocrystalline AlN thin films, *Thin Solid Films*, Vol. 251(2), pp. 121-126.
- Xu, X.H., Wu, H.S., Zhang, C.J. & Jin Z.H. (2001). Morphological properties of AlN piezoelectric thin films deposited by DC reactive magnetron sputtering, *Thin Solid Films*, Vol. 388, pp. 62-67.
- Yamada, H., Ushimi, Y., Takeuchi, M., Yoshino, Y., Makino, T. & Arai, S. (2004). Improvement of crystallinity of ZnO thin film and electrical characteristics of film bulk acoustic wave resonator by using Pt buffer layer, *Vacuum*, Vol. 74, pp. 689-692.
- Yim, W.M., Stofko, E.J., Zanzucchi, P.J., Pankov, J.I., Ettenberg, M. & Gilbert, S.L. (1973). Epitaxially grown AlN and its optical band gap, *J. Appl. Phys.*, Vol. 44(1), pp. 292-296.



Acoustic Waves - From Microdevices to Helioseismology

Edited by Prof. Marco G. Beghi

ISBN 978-953-307-572-3

Hard cover, 652 pages

Publisher InTech

Published online 14, November, 2011

Published in print edition November, 2011

The concept of acoustic wave is a pervasive one, which emerges in any type of medium, from solids to plasmas, at length and time scales ranging from sub-micrometric layers in microdevices to seismic waves in the Sun's interior. This book presents several aspects of the active research ongoing in this field. Theoretical efforts are leading to a deeper understanding of phenomena, also in complicated environments like the solar surface boundary. Acoustic waves are a flexible probe to investigate the properties of very different systems, from thin inorganic layers to ripening cheese to biological systems. Acoustic waves are also a tool to manipulate matter, from the delicate evaporation of biomolecules to be analysed, to the phase transitions induced by intense shock waves. And a whole class of widespread microdevices, including filters and sensors, is based on the behaviour of acoustic waves propagating in thin layers. The search for better performances is driving to new materials for these devices, and to more refined tools for their analysis.

How to reference

In order to correctly reference this scholarly work, feel free to copy and paste the following:

Jyoti Prakash Kar and Gouranga Bose (2011). Aluminum Nitride (AlN) Film Based Acoustic Devices: Material Synthesis and Device Fabrication, *Acoustic Waves - From Microdevices to Helioseismology*, Prof. Marco G. Beghi (Ed.), ISBN: 978-953-307-572-3, InTech, Available from: <http://www.intechopen.com/books/acoustic-waves-from-microdevices-to-helioseismology/aluminum-nitride-aln-film-based-acoustic-devices-material-synthesis-and-device-fabrication>

INTECH
open science | open minds

InTech Europe

University Campus STeP Ri
Slavka Krautzeka 83/A
51000 Rijeka, Croatia
Phone: +385 (51) 770 447
Fax: +385 (51) 686 166
www.intechopen.com

InTech China

Unit 405, Office Block, Hotel Equatorial Shanghai
No.65, Yan An Road (West), Shanghai, 200040, China
中国上海市延安西路65号上海国际贵都大饭店办公楼405单元
Phone: +86-21-62489820
Fax: +86-21-62489821

© 2011 The Author(s). Licensee IntechOpen. This is an open access article distributed under the terms of the [Creative Commons Attribution 3.0 License](#), which permits unrestricted use, distribution, and reproduction in any medium, provided the original work is properly cited.

IntechOpen

IntechOpen